Pacific Northwest
NATIONAL LABORATORY

PNNL-33528

Building Model Calibration: Validation of GridLAB-D Thermal Dynamics Modeling

November 2022

Carolyn D Goodman
Laura E Hinkle
Trevor D Hardy
Hayden M Reeve

U.S. DEPARTMENT OF ENERGY

Prepared for the U.S. Department of Energy
under Contract DE-AC05-76RL01830

DISCLAIMER

PACIFIC NORTHWEST NATIONAL LABORATORY
operated by
BATTELLE
for the
UNITED STATES DEPARTMENT OF ENERGY
under Contract DE-AC05-76RL01830

Printed in the United States of America

Available to DOE and DOE contractors from the
Office of Scientific and Technical Information,
P.O. Box 62, Oak Ridge, TN 37831-0062;
ph: (865) 576-8401
fax: (865) 576-5728
email: reports@adonis.osti.gov

Available to the public from the National Technical Information Service
5301 Shawnee Rd., Alexandria, VA 22312
ph: (800) 553-NTIS (6847)
email: orders@ntis.gov <https://www.ntis.gov/about>
Online ordering: http://www.ntis.gov

Building Model Calibration: Validation of GridLAB-D Thermal Dynamics Modeling

November 2022

Carolyn D Goodman
Laura E Hinkle
Trevor D Hardy
Hayden M Reeve

Prepared for
the U.S. Department of Energy
under Contract DE-AC05-76RL01830

Pacific Northwest National Laboratory
Richland, Washington 99354

Abstract

This report investigates how well GridLAB-D's house model characterizes the thermal dynamics of buildings given the overpredicted diurnal electric load swing observed in the Distribution System Operation with Transactive (DSO+T) study. This study seeks to validate GridLAB-D's house model by calibrating it to data from the well-instrumented Pacific Northwest National Laboratory Lab Homes in Richland, WA. The datasets chosen included multiple pre-cooling and pre-heating testing periods where the indoor air temperature was allowed to float over a multi-hour length of time to mimic diurnal behavior. The multi-season calibrations were evaluated by comparing the heating/cooling electric power, indoor air temperature, and the rise/decay time during temperature float periods with Lab Homes data. The default GridLAB-D assumptions for latent load fraction, air heat capacity, mass heat capacity, window-to-wall-ratio, overall envelope conductance (assumed as NORMAL thermal integrity level), and solar heat gain coefficient were compared with the calibrated model to confirm when the default assumptions were adequate and the impact of calibration on the accuracy of modeling the thermal dynamics of homes.

Summary

The purpose of the building model calibration study in GridLAB-D was to investigate how well GridLAB-D's house model characterized the thermal dynamics of buildings given the overpredicted diurnal electric load swing observed in the Distribution System Operation with Transactive (DSO+T) study. This study seeks to validate GridLAB-D's house model by calibrating it to data from the well-instrumented Pacific Northwest National Laboratory Lab Homes in Richland, WA. The datasets chosen included multiple pre-cooling and pre-heating testing periods where the indoor air temperature was allowed to float over a multi-hour length of time to mimic diurnal behavior. The calibration was completed over three test periods (in August, June, and December) to mitigate overfitting and evaluate seasonal effects on the parameter choices for air heat capacity, mass heat capacity, window-to-wall ratio (WWR), overall envelope conductance (UA value), solar heat gain coefficient (SHGC), and latent load fraction.

Calibration was completed by identifying the parameter value combination that minimized the mean squared error (MSE) for indoor air temperature (IAT) or heating/cooling electric power during each representative time period. An overall calibration was completed by calculating the IAT and heating/cooling electric power MSE for each season and combining them to a singular value using a weighted average such that summer and winter were twice as important as spring, given the difficulty of fitting shoulder month data. The parameter grid search calibration method was chosen to observe trends between parameter selection and model performance. A sensitivity analysis was conducted by using the overall calibration as the baseline, and varying individual calibration parameters to quantify the effects on the heating/cooling electric power MSE and on the rise or decay time error during the temperature float events. To validate GridLAB-D's default assumptions were adequate to characterize a home's thermal dynamics, a model with GridLAB-D's default assumed value for the six calibration parameters was compared throughout the study. The comparison with GridLAB-D's default assumptions aimed to show the impact of calibration and indicate if GridLAB-D's default assumptions should be improved.

The GridLAB-D calibrations across all seasons closely predicted the indoor air temperature and the rise/decay times. The summer, winter, and spring power calibrations predicted the total heating/cooling electricity consumption with a 13% error, 5% error, and -17% error respectively. The summer calibration parameter sets trended towards a higher air heat capacity to dampen indoor air temperature fluctuations and a lower mass heat capacity to prevent overprediction of the rise times. The winter calibration parameter set resulted in a higher mass heat capacity and a high integrity envelope due to a long 14-hour decay period that GridLAB-D underpredicted. The large percent error during the 14-hour decay period may have been due to inaccurate heat gain measurements in the Lab Home. The short decay periods in the winter were modeled within 25 minutes of the Lab Home dataset. The spring calibration also selected a higher mass heat capacity and a high integrity envelope due to long periods where the heat pump was off and the indoor air temperature was maintained. The error during the spring test period could be due to incorrect estimation of solar gains or unmeasured internal gains. A lower latent load fraction than the default GridLAB-D assumption was selected in the summer and spring calibrations to minimize both IAT and power MSE. Given that Richland, WA is a dry climate, this was expected.

From analyzing the rise/decay time results and the overall goal of this study to accurately simulate the thermal dynamics of a house during setpoint changes, the overall heating/cooling power calibration was the recommended parameter set. The overall calibration parameter set reduced the total absolute electricity error from 45% to 5.7% compared to the model that used GridLAB-D's default assumptions for the six testing parameters. The GridLAB-D default model underpredicted the rise/decay time because of the low mass heat capacity value. The GridLAB-D default model was also more thermally responsive due to the higher overall UA

value than the calibrated model. In general, the GridLAB-D default model performed worse during very high and very low temperatures emphasizing the importance of correct thermal parameter definitions for resilience testing or extreme weather studies.

The sensitivity analysis indicated that the power MSE was most sensitive to changes to the UA value. The rise/decay time error was more sensitive to changes to the air and mass heat capacity but was most sensitive to modifications to the building envelope (UA value, WWR, and SHGC). GridLAB-D models the thermal mass with a lumped capacitance method. Further validation of this method on buildings with more massive exterior walls may produce different findings for the sensitivity analysis and merits investigation. The power MSE and the rise/decay time error were also not sensitive to changes to the latent load fraction. Because GridLAB-D accounts for the latent load by adjusting the sensible cooling capacity based on outdoor humidity rather than with a moisture balance, the latent load fraction is less impactful in a climate like Richland, WA where the relative humidity is low during cooling season.

GridLAB-D's modeling capabilities are likely not the cause of the overpredicted diurnal electric load change and most likely due to inaccurate building population parameter distributions (schedules, exterior wall material, etc.) or other assumptions made about non-building loads. Future work should thoroughly investigate the impact of GridLAB-D's latent load fraction in high humidity climates and GridLAB-D's thermal mass simplification on buildings with massive exterior façades.

Contents

Figures

Tables

1.0 Background

With the ever increasing complexity of the electric grid associated with electricity supply from renewable sources and the use of distributed energy resources, it is critical that simulation tools are efficient and accurate when simulating various control strategies and scenarios. *GridLAB-D* (2020) is a power system simulation technology that enables users to model end-use loads coupled with power system analysis for smart grid evaluation. GridLAB-D was recently used in the Distribution System Operator with Transactive (DSO+T) study which designed and simulated a transactive energy retail market coordination scheme for the Texas grid (Reeve et al. 2022). A key finding from the GridLAB-D modeled aggregate load profiles compared to 2016 ERCOT system load data was a high overprediction of the daily load variation (about 42% on average). An extensive effort was made to estimate thermal parameters for the ERCOT residential and commercial building populations. However, because heating, ventilation, and air conditioning (HVAC) accounts for about 25% of the annualized distribution system load and demonstrates a high diurnal swing during typical operations (Reeve et al. 2022), the accuracy of the building models could be one source of error. If the thermal dynamics are not appropriately modeled, the building's thermal decay or rise time may be too long or short and contribute to the high diurnal swing. In addition, GridLAB-D varies the latent load only with outdoor air relative humidity, without incorporating envelope integrity or internal relative humidity levels, which is not consistent with real world HVAC loads. This study examines if GridLAB-D and the default assumptions associated with the house model should be improved to better characterize thermal dynamics through calibration with real home data.

GridLAB-D's residential module consists of a thermal heat flow circuit otherwise known as an equivalent thermal parameter (ETP) model (Figure 1) (*GridLAB-D* 2017). It is simple, efficient, and well vetted to accurately represent residential thermal behavior and energy consumption (Sonderegger 1978, Subbarao 1981, N. Wilson et al. 1985). Various studies have used GridLAB-D and the underlying residential load model to simulate demand response strategies and power system analysis. Schneider and Fuller (2010) used detailed residential models in GridLAB-D to demonstrate the impact of end-use loads on electricity distribution systems. Gotseff and Lundstrom (2017) calibrated GridLAB-D house models with aggregate summer load data for a group of 10 homes. The study tuned the models using the qualitative *thermal_integrity_level* GridLAB-D parameter to characterize the house insulation level and the *cooling_COP* GridLAB-D parameter to define the coefficient of performance (COP) for the cooling system. Because only aggregate load data was available rather than the HVAC load and internal temperature for each home, a non-HVAC load profile was also defined to complete the calibration. Results indicated a less than 5% difference in daily average energy and similar load shape. Zhou et al. (2019) studied demand response strategies for 2000 air conditioners modeled in GridLAB-D. Demand response was evaluated during both the load reduction/load shed phase and during the temperature recovery stage after the demand response event with the goal of restoring temperature and minimizing load spikes. The residential house models were not validated against real home data.

The diurnal swing overprediction observed in DSO+T (Reeve et al. 2022) is also present in population scale EnergyPlus modeling completed in Hale et al. (2018). Modeling of residential, commercial, industrial, and transportation end-loads were compared with actual 2012 grid loads with building models informed by ResStock and ComStock databases. Accuracy of the results increased from a 20% error at an hourly resolution to a 4% error at an annual resolution. The daily swing overprediction present in the EnergyPlus models indicates improving the fidelity of GridLAB-D's modeling approach may not address the underlying problem with characterizing the daily load. In addition, calibration of EnergyPlus models is often completed using total energy consumption at longer time resolutions (daily to annual scale rather than second to minute

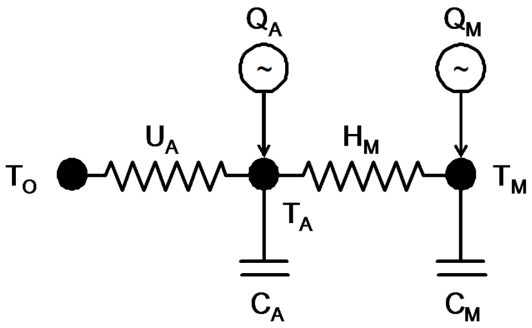

Figure 1. Equivalent Thermal Parameters Circuit Modeled by House-E in GridLAB-D (2020)

scale) than necessary to capture the thermal dynamics of buildings. The shorter time resolution is necessary for grid modeling/power systems analysis and where GridLAB-D bridges the gap.

Although the ETP model has been validated against actual home data and other studies use GridLAB-D's ETP model to define end-use loads, few have thoroughly investigated how GridLAB-D's House_E model performs during extreme setpoint changes which tests the limits of the simple thermal mass description in the ETP circuit. In addition, some GridLAB-D parameters have default values with unclear origins and therefore, require validation against data. Lastly, GridLAB-D's inclusion of the latent load has not been validated as it is not present in the original ETP model. By calibrating a GridLAB-D house model with data from a well-instrumented house, this study outlines if there are possible areas of improvement for GridLAB-D's residential model in order to mitigate accuracy problems at scale.

2.0 GridLAB-D Methodology

Although the focus of GridLAB-D is power system simulation, the user can define a residential house model to varying levels of fidelity. Parameters can be defined with a categorical value or with a more specific numeric entry (which is the method used in this study). As mentioned in Section 1.0, GridLAB-D's House_e model is based on an ETP model (see Figure 1). The parameters in the ETP model are defined below:

- U_A: house envelope (walls, windows, doors, ceilings, floors, and infiltration) overall conductance
- T_O: outdoor air temperature
- T_A: indoor air temperature
- T_M: thermal mass temperature
- C_M: lumped thermal mass
- C_A: thermal mass of the air
- H_M: interior mass surface conductance
- Q_A: heat delivered to the air
- Q_M: heat delivered to the mass

GridLAB-D incorporates electricity consumption and heat gains from lighting, plug loads, appliances, and occupants through the use of ZIPLoads. For a thorough explanation of the House_e model in GridLAB-D, review the Residential Module User Guide (*GridLAB-D* 2017). The parameters of interest for this study include the rated latent load fraction (%), the air heat capacity (C_A, BTU/°F), the mass heat capacity (C_M, BTU/°F), the window-to-wall ratio (WWR, %), the overall envelope conductance (U_A, BTU/°F-hr), and the window shading factor/solar heat gain coefficient (SHGC, %).

2.1 Latent Cooling Load

GridLAB-D incorporates an approximation of the latent load. By default, the rated latent cooling fraction of sensible cooling is 30% which translates to a fractional increase in the design cooling load due to the latent cooling requirements. Rather than complete a moisture balance to determine the latent load at each timestep, the latent cooling fraction is adjusted based the outdoor relative humidity (see Equation 1).

$$LatentLoad_{frac,adj.} = \frac{0.1 + LatentLoad_{frac,rated}}{1 + exp(4 - 10RH_{out})} \quad (1)$$

The adjusted latent cooling fraction discounts the total cooling capacity of the system. The cooling power in GridLAB-D is only applied to the sensible cooling load, so discounting the cooling capacity is required to ensure the sensible cooling capacity isn't overestimated. Figure 2 shows how the adjusted latent load fraction is impacted by the outdoor relative humidity. As the outdoor humidity increases, the difference between high and low rated latent load fractions increases. When the relative humidity is 21%, the adjusted latent load fraction is between 11%

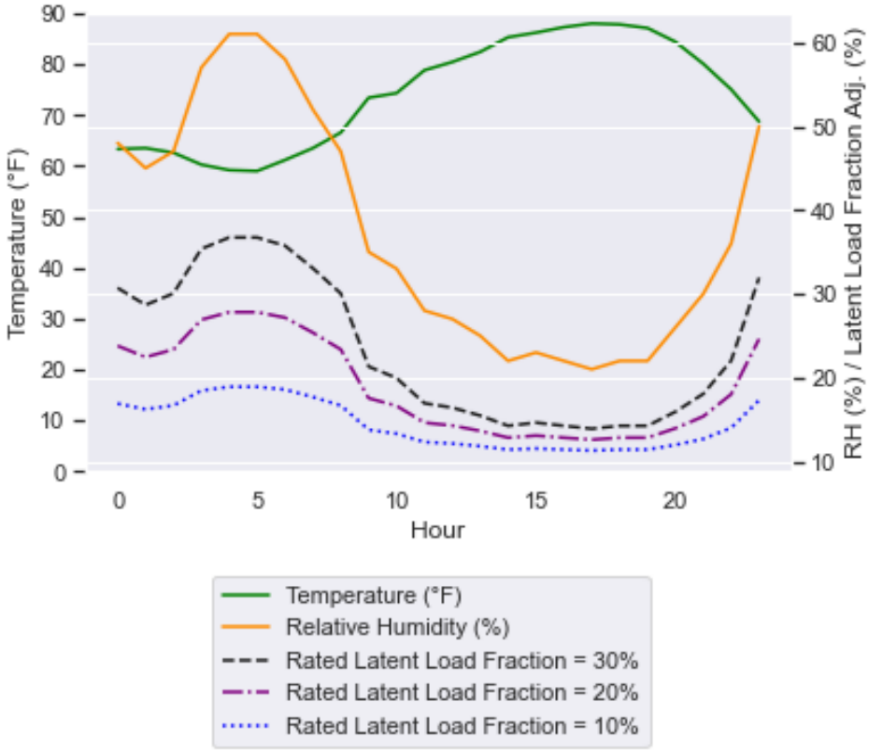

Figure 2. Adjusted latent load fraction for three different rated latent load fractions in Richland, WA on July 18, 2022

and 14% for the plotted rated latent latent load fractions. When the outdoor relative humidity is 61%, the adjusted latent load fraction ranges from 19% to 37% depending on the rated latent load fraction. Choosing an appropriate rated latent load fraction impacts the sensible cooling capacity more in a humid climate than in a dry climate. Because GridLAB-D does not complete a moisture balance at each timestep, the adjusted latent load fraction based only on outdoor air humidity could overestimate or underestimate the latent cooling load in a building. Outdoor relative humidity is usually higher at night and therefore mischaracterizing the rated latent load fraction could contribute to the high diurnal swing observed in the DSO+T study (Reeve et al. 2022). Without the moisture balance, GridLAB-D fails to capture dehumidification requirements when the indoor thermostat setpoints are met but the indoor relative humidity is above 55% (the typical acceptable high limit for indoor relative humidity). This is more likely to occur at night when the outdoor temperature is lower, but the outdoor relative humidity is higher and when more residential occupants are likely to be inside contributing to the latent load.

2.2 Air Heat Capacity

The air heat capacity in GridLAB-D is responsible for the dampening the indoor air temperature changes due the heating and cooling system, otherwise known as the short-cycle thermal mass (*GridLAB-D* 2017). In GridLAB-D, the air mass includes surface effects from the mass as well, therefore the air heat capacity is larger in GridLAB-D than the physical property. GridLAB-D documentation notes that the air heat capacity is well approximated as three times the volumetric capacitance of the interior air volume. There is no reference for the air heat capacity

approximation. Because both the air mass and the solid thermal mass contribute to the long term thermal dynamics in a building and due to the lack of reference material for the calculation, this study used air mass as one of the calibration tuning parameters.

2.3 Thermal Mass Heat Capacity

The typical method of defining the thermal mass heat capacity in GridLAB-D is to define the total thermal mass per unit floor area (Btu/°F-ft^2). The total thermal mass (C_M) used for the longer cycle mass is calculated by multiplying the total thermal mass per unit floor area minus the extra two ”air” thermal mass units added to the air heat capacity. In order to be straightforward with the calibration process, the C_M value was set directly, decoupling its calculation from the air heat capacity estimate.

2.4 Overall Envelope Conductance

GridLAB-D sums all the parallel heat flows through the envelope into the building to determine the U_A value, including infiltration but excluding solar heat gains. Although U_A can be estimated from thermal integrity values for walls, ceilings, and floors, it was used for calibration to evaluate the major contributors of the ETP model.

2.5 Window-to-Wall Ratio and Solar Heat Gain Coefficient

GridLAB-D does not accept different WWRs for each façade. The defined WWR is applied to all sides of the building to calculate the gross window area. The gross window area multiplied by the solar radiation, the glazing SHGC, and the window exterior transmission coefficient (defaulted to 0.6) determines the solar heat gain for the building. Because the window exterior transmission coefficient (the coefficient for the amount of energy passing through a window) is unknown, an effective glazing SHGC value is estimated through the calibration process and accounts for interior and exterior shading effects not explicitly included in the House_e model. Although the effects of singular WWR value may average out at scale, determining an effective WWR for calibrating one home is important to understand the effect of the other parameters of interest. There may be some non-linear distortions of HVAC loads in buildings with predominantly north-south or east-west window orientations that don’t average out at population scale, but that is beyond the scope of this study.

3.0 Model Calibration

To determine the accuracy of GridLAB-D's house model from a thermal dynamics perspective, a fully calibrated model was required. This section will discuss the calibration process in detail.

3.1 House Thermal and Power Data Source

Pacific Northwest National Laboratory (PNNL) has two custom factory-built double-wide homes that are well-instrumented to conduct residential load research (*PNNL: Lab Homes* 2022). Data collectors for the two identical lab homes collect data for a variety of measurements including indoor air temperature, outdoor air temperature, solar insolation, and power consumption for each circuit in the homes at sub-minute intervals. In order to fully test the fidelity of GridLAB-D's house thermal dynamics modeling and to prevent overfitting, datasets from summer, winter, and spring were selected. This study relied on previously conducted experiments for data and therefore, the time range was limited for each test period. For each data collection period, this study used outdoor air temperature (°F), indoor air temperature (°F), thermostat setpoint (°F), HVAC power consumption (W), and solar insolation (W/m^2). Simulated occupancy loads using heaters were in use during the winter and spring datasets, so the heat power consumption was also included in the GridLAB-D models as an internal heat gain (modeled as a heat gain only ZIPload).

Table 1 outlines the applicable characteristics of the Lab Home obtained from *PNNL: Lab Homes* (2022) along with nameplate data for HVAC equipment. This includes the Seasonal Energy Efficiency Ratio (SEER) and the Heating Seasonal Performance Factor (HSPF). The conditioned floor area, ceiling height, and aspect ratio were derived from an EnergyPlus model for the Lab Homes (Metzger et al. 2017). The floor area, aspect ratio, ceiling height, and heating and cooling capacity (for the heat pump and the electric furnace) were explicitly defined in GridLAB-D and held constant for all simulations. The number of stories was set to *1*. The fan type was set to "TWO_SPEED". The HVAC performance values were converted to a rated coefficient of performance (COP) and defined explicitly for both heating and cooling. The rated COP was held constant for all simulations. Calibration of the COP beyond the rated value was not completed as the timing of the heat pump cycles was more important for this study than the magnitude of the heat pump power consumption. GridLAB-D adjusts the COP at each timestep based on the outdoor air temperature. All other parameters beyond the calibration parameters (see Section 3.3.1) and values outlined above used GridLAB-D default assumptions. Refer to *GridLAB-D* 2017 for more information on COP adjustment and GridLAB-D's default assumptions.

Datasets were selected where the temperature was allowed to float between two thermostat setpoints. The primary driver of this investigation was the high diurnal electrical load swing demonstrated in the DSO+T simulations which could be due to inaccurate modeling of the building thermal behavior during night setback (increasing the cooling setpoint or decreasing the heating setpoint at night). Therefore, pre-heating and pre-cooling datasets are appropriate tests to validate GridLAB-D's thermal dynamics during the period when the temperature floats.

3.1.1 Summer Dataset

A key starting point for the Lab Homes analysis in GridLAB-D included review of Rogers and Brambley (2021) which calculated the thermal parameters of the Lab Homes during August 2020 using pre-cooling tests. The thermostat cooling setpoint was changed between 68°F and

Table 1. PNNL Lab Homes Characteristics

Parameter	Value
Floor Area	1493 ft^2
HVAC Type	Central heat pump with fan wall heaters
HVAC Performance	13 SEER/8 HSPF
Heat Pump Cooling Capacity	29,400 BTUH
Heat Pump Heating Capacity	30,000 BTUH
Aux. Electric Furnace Heating Capacity	53,000 BTUH
Window Area	195.7 ft^2
Thermal Integrity	Floors: R-22
	Walls: R-11
	Ceiling: R-22
Ceiling Height	8.502 ft
Aspect Ratio	1.91

78°F to analyze the rise time and the thermal storage potential of the Lab Home. The parameters of interest were thermal capacitance (*C*) and the heat transfer coefficient (*UA*). The energy balance equation to calculate the thermal parameters is

$$C\frac{\partial T}{\partial t} = Q_c + UA(T_o - T) \tag{2}$$

where *T* is the indoor air temperature, *t* is time, T_o is the outdoor air temperature, and Q_c is the cooling capacity of the heat pump. The UA value calculated is an effective overall heat transfer coefficient that incorporates infiltration and solar gains which weren't explicitly modeled. GridLAB-D does model solar gains so the heat transfer coefficient and thermal capacitance from the Thermal Parameters study were only used initially. Data driven calculations resulted in a thermal capacitance of 3870 Btu/°F and a heat transfer coefficient of 580 Btu/hr-°F. Rogers and Brambley (2021) also estimated properties for a research home at the University of Oklahoma (OU). Unfortunately, the heat pump power data quality was poor and therefore, not a candidate dataset for the GridLAB-D calibration. A preliminary calibration was completed for the OU home to evaluate the effects of a brick exterior thermal mass and a high humidity climate. The results are in Section 5.0.

The GridLAB-D study in this report used data from August 18, 2020 through August 20, 2020. Outdoor air temperature varies from 67°F to 102°F. Three pre-cooling tests were included in this three-day dataset with each test period starting at 3 PM when the heat pump shut off and the temperature increased to the elevated cooling setpoint (from 68°F to 78°F). The latent load modeling is a value of interest for this investigation. The outdoor relative humidity varied from 25% to 81%. Although this is a large swing, the absolute humidity is more constant due to the variable dry bulb temperature leading to a more constant "humidity" gain via infiltration. The relatively constant absolute outdoor humidity is not reflected in GridLAB-D's latent load modeling.

3.1.2 Winter Dataset

A pre-heating test was conducted in the Lab Home from December 15, 2021 through December 21, 2021. The outdoor air temperature varied from 14°F to 53°F. The heating setpoint varied from 55°F to 76°F. Two small pre-heating tests were conducted on December 17, 2021 and December 19, 2021 where the thermostat setpoint dropped from 76°F to 68°F. Two additional small pre-heating tests on December 18, 2021 and December 20, 2021 dropped the heating setpoint from 74°F to 70°F. All small pre-heating test periods started at 6 AM when the heat pump shut off and the temperature decreased to the reduced heating setpoint. One extreme pre-heating test on December 21, 2021 reduced the thermostat setpoint from 76°F to 55°F. The heating setpoint dropped from 76°F to 55°F at midnight on December 21, 2021 and remained at 55°F for the whole day.

It is important to note some potential error for the power measurement in the pre-heating Lab Home dataset. There were multiple instances where power measurements indicated the heat pump was running, but the indoor air temperature measurement showed the house indoor air temperature was decreasing. After examining the data more closely, specifically during the pre-heating/decay test, it was determined that the power data was off by one hour. For example, on December 17th at 6 AM when the setpoint dropped from 76°F to 68°F, the power data indicated the heat pump continued to cycle on and off until 7 AM before shutting off. The indoor air temperature decreased continuously between 6 AM and 7 PM indicating the heat pump was actually off during that period, following the reduced heating setpoint. Given these findings, the power data was shifted backwards by one hour for this analysis. Power measurements include both the heat pump and the auxiliary electric furnace power consumption.

3.1.3 Spring Dataset

A pre-cooling test was conducted in the lab home from June 9, 2022 to June 13, 2022. The outdoor air temperature varied from 50°F to 86°F. The cooling setpoint varied from 68°F to 78°F similar to the pre-cooling tests in Section 3.1.1. No heating was used during this test period. Pre-cooling test periods were from 6 AM to 10 AM and 2 PM to 7 PM each day (when the cooling setpoint increased from 68°F to 78°F). Only the pre-cooling test periods at 2 PM were analyzed in this report. The outdoor air temperature was less extreme in June because it was the shoulder season. Therefore, the heat pump was off for longer periods of time and deviation from the cooling setpoint was minimal when the heat pump was off. On June 12, 2022 and June 13, 2022, the outdoor air temperature was less than 65°F and so the indoor air temperature decayed similar to the pre-heating tests. On June 13, 2022, the heat pump never turned on because the indoor temperature was less than the cooling setpoint. After review data from the test period, June 9, 2022 through June 11, 2022 are classified as pre-cooling tests while June 12, 2022 and June 13, 2022 are classified as free floating internal air temperature tests.

3.2 Weather Data

GridLAB-D requires weather data in TMY (typical meteorological year) format. The Lab Home calibrated in GridLAB-D is located in Richland, WA. The TMY3 weather file for Pasco, WA was used as the starting point GridLAB-D weather file and updated with actual weather data from each test period to accurately calibrate the GridLAB-D model. Outdoor dry-bulb temperature, outdoor relative humidity percentage and Global Horizontal Irradiation (GHI W/m^2) were replaced in the TMY3 file for the three time periods tested (August, June, and December). All

other values were left as the default for the weather file. The GridLAB-D house model only uses outdoor air dry-bulb temperature, outdoor air relative humidity, and solar flux data from the TMY files so replacing those values is sufficient for this calibration exercise.

3.3 Calibration Process

3.3.1 GridLAB-D Calibration

The GridLAB-D house model was calibrated by identifying the combination of parameter values that minimized the mean squared error (MSE) for indoor air temperature or HVAC electric power during each representative time period. An overall calibration was completed by calculating the IAT and HVAC electric power MSE for each season and combining them to a singular value using a weighted average such that summer and winter were twice as important as spring, given the difficulty of fitting shoulder month data. The overall parameter set was identified by selecting the lowest weighted MSE for the cooling power and IAT. Six parameters were varied during calibration: air heat capacity, rated latent load fraction, mass heat capacity, window-to-wall ratio, overall envelope conductance, and SHGC (see Table 2). A parameter grid approach was used in order to understand the sensitivities of each variable. The parameter grid search also allows for more straightforward comparison between each seasonal calibration. The chosen parameters were hypothesized to impact the GridLAB-D's thermal response during extreme conditions. For each parameter, a discrete number of values was selected based on GridLAB-D defaults and PNNL Connected Homes Impact of Thermal Parameters Study (Rogers and Brambley 2021). The default air thermal mass value in GridLAB-D is $3 * C_{p,air} * m_{air}$, which equates to 672.6 BTU/°F using GridLAB-D's default values. In Rogers and Brambley (2021), the estimated latent load fraction was 0.10, and the estimated mass heat capacity was 3780 BTU/°F. GridLAB-D does not accept a WWR to each façade. The Lab Home windows vary around the building, therefore, the appropriate effective whole building WWR was included along with the glazing SHGC. The overall estimated envelope conductance was 580 BTU/°hr-F from Rogers and Brambley (2021). In GridLAB-D, the envelope conductance includes both the envelope and infiltration.

It was understood after the calibration process that individually calibrating the WWR and SHGC does not make sense in GridLAB-D as they are simply multiplied together with the solar radiation, window exterior transmission coefficient, and building surface area to determine the solar heat gain. The relation of the two parameters is mentioned throughout the results but is noted here for clarity.

Table 2. GridLAB-D Parameter Grid

Parameter	Options
Latent load fraction	5%, 10%, 15%
Air heat capacity (BTU/°F)	600, 800, 1000, 1200
Mass heat capacity (BTU/°F)	3580, 3780, 3980, 4180
Window-to-wall ratio	5%, 10%, 15%
Overall Envelope Conductance (UA) (BTU/°F-hr)	380, 580, 780, 980
SHGC	20%, 40%, 60%, 80%

3.3.2 Default GridLAB-D Parameters

GridLAB-D allows a house to be defined with only a few parameters. At the population scale, calibration of individual homes is not possible and some important thermal parameters may be unknown. In order to quantify the importance of calibration in the building stock, validation of GridLAB-D's default assumptions were compared with the parameter grid search calibration (outlined in Section 3.3.1). Future work includes further validation of GridLAB-D's default assumptions, outside the calibration parameters in this study, on other residential datasets. Parameter values for the six parameters varied during calibration were given the default GridLAB-D assumptions. All other values used to define the home were left the same as the calibrated model. Table 3 outlines the default values in GridLAB-D. Instead of setting the mass heat capacity directly, the total thermal mass per floor area was set to 2.0 BTU/°F-ft^2 which GridLAB-D documentation says represents residential wood-frame construction including furnishings. The thermal mass per floor area resulted in a mass heat capacity of 2539 BTU/°F. This lower mass heat capacity was not included in the parameter grid search because the Thermal Parameters Study (Rogers and Brambley 2021) indicated the Lab Home's thermal mass was likely around 3800 BTU/°F. The UA and the SHGC were set by a thermal integrity level categorical value of "NORMAL". "NORMAL" was used here to represent a typical home. GridLAB-D's default assumptions were used for the WWR, rated latent load fraction, and the air heat capacity.

Table 3. Default GridLAB-D Parameters

Parameter	Options
Latent load fraction	30%
Air heat capacity (BTU/°F)	672.61
Mass heat capacity (BTU/°F)	2538.97
Window-to-wall ratio	15%
Overall Envelope Conductance (UA) (BTU/°F-hr)	593.526
SHGC	67%

4.0 Results

4.1 Calibration Results

The Lab Home GridLAB-D model parameters were calibrated using two approaches; 1) minimizing the mean squared error (MSE) for indoor air temperature (IAT), and 2) minimizing the MSE for cooling or heating electric power. The representative time period for each season was calibrated, and subsequent calibration was done across all seasons with the MSE of each season weighted to provide an overall recommendation (see Table 4). The summer and winter MSE were weighted at 0.4 while the spring MSE was weighted at 0.2. Refer to Section 3.3.1 for information on the parameter grid search. Throughout the results, when cooling power, heating power, or HVAC power is mentioned, it is referring to electric power used by the heat pump and auxiliary electric furnace to perform heating or cooling.

4.1.1 Summer Calibration

The rise times for the summer pre-cooling tests are shown in Table 5. Plots of the IAT, OAT, the cooling electric power for the Lab Home and the GridLAB-D model are shown in Figure 3 for the cooling power calibration and IAT calibration.

The power plot in Figure 3 shows an obvious difference in magnitude between the model and the dataset. Although the COP could have been calibrated in order to better match the power measurements, it was ultimately decided to remain focused on the thermal parameters only and leave the COP at the rated value. There may be issues in the magnitude of the power measurements (possibly the power data measuring an additional fan not included in the GridLAB-D model) or the heat pump efficiency may have decreased with age resulting in higher power consumption. The cooling power in GridLAB-D matches the input COP based on the rated cooling capacity indicating this is not a GridLAB-D modeling issue.

Compared to the IAT calibration, the UA value was higher for the cooling power calibration parameter set while the WWR and SHGC were lower potentially canceling out some heat gain effects. The cooling power calibration resulted in a higher air heat capacity compared to the IAT calibration. The IAT calibration matched the rise times of the dataset more closely than the cooling power calibration with a 6% combined error and a 27% combined error respectively. Most of the rise time error in the cooling power calibration originates from the third pre-cooling test. During the third pre-cooling test on August 20th, the outdoor air temperature was lower (at about 90°F), and the cooling power calibration rise time was 45-minutes longer than the IAT calibration. This indicates a potential switch point where at more mild outdoor air temperatures, the heat capacity of the air and mass have a larger effect on rise time because the envelope heat gains are less extreme. This is evident during the mornings of August 19th and 20th. The outdoor air temperature was lower during the mornings of August 19th and 20th, allowing the internal air temperature to float without the use of HVAC. In order for the IAT calibration to maintain the internal air temperature during these periods, the heat pump turned on about an hour earlier than the cooling power calibration. The IAT calibration used a lower air heat capacity than the cooling power calibration. Therefore, the amount of time the heat pump could remain off was generally lower.

Even with the higher overall envelope conductance in the cooling power calibration, the solar heat gains are greatly reduced by the lower WWR and SHGC. The cooling power calibration model experienced 22% of the solar heat gains that the IAT calibration model experienced which helps explain the lower total energy consumption (more negative energy error). The higher UA-value effect (in the cooling power calibration) was more evident at night at lower

Table 4. Calibration Results

Season	**Result type**	Latent Load Fraction	Air heat capacity (BTU/°F)	Mass heat capacity (BTU/°F)	WWR	UA (BTU/°F-hr)	SHGC	Weighted IAT ($°F^2$)/ Power (kW^2) MSE	HVAC electricity error
Summer	Lowest IAT MSE	5%	800	3580	15%	580	60%	0.73	-11.2%
	Lowest cooling power MSE	10%	1000	3580	5%	780	40%	1.08	-12.7%
Winter	Lowest IAT MSE	-	1200	4180	5%	380	60%	0.98	0.08%
	Lowest heating power MSE	-	800	4180	10%	380	40%	9.81	4.9%
Spring	Lowest IAT MSE	5%	1200	4180	15%	380	40%	0.92	-56.6%
	Lowest cooling power MSE	15%	800	4180	15%	580	80%	0.41	-17.0%
Overall	Lowest IAT MSE	15%	1200	4180	15%	380	40%	1.34	-8.8%
	Lowest power MSE	10%	1000	4180	15%	380	80%	4.57	-5.7%
Overall	Default	30%	673	2539	15%	594	67%	$3.43°F^2$ $4.46kW^2$	45%

outdoor air temperatures where Figure 3 shows the indoor air temperature was more thermally responsive when compared to the IAT calibration.

The IAT calibration resulted in a lower rated latent load fraction than the cooling power calibration. This is likely related to the reduced cooling load experienced by the cooling power calibration model due to the reduced solar heat gains. In order to match the power draw with the lower cooling load, less of the cooling capacity was used for sensible cooling. Both calibration efforts resulted in a rated latent load fraction smaller than the 30% default value. The lowest error compared to the Lab Home dataset was when almost all of the cooling capacity was used for sensible cooling in GridLAB-D. A 5% rated latent load fraction when adjusted in GridLAB-D using the method outlined in Section 2.1 resulted in an adjusted latent load fraction from 1% to 14%. The higher adjusted latent cooling fraction would occur on August 19th and August 20th at 6 AM which was when the cooling system was off, therefore the latent load minimally impacts the cooling power. When the cooling system was on, the adjusted latent load fraction was less than 10%. Because of the calculation method for the adjusted latent load fraction, the 10% rated latent load fraction was not significantly different than the 5% rated latent load fraction during heat pump runs. This will be further discussed in Section 4.3.

Compared to the Lab Homes dataset, the error metrics are low for both the IAT focused study and the cooling power focused study, indicating good calibration.

Table 5. Rise time during summer period

Pre-cool event	Result type	GridLAB-D rise time (hr)	Lab home rise time (hr)
08/18 3:00 PM	Lowest IAT MSE	01:50	01:50
	Lowest cooling power MSE	01:55	-
08/19 3:00 PM	Lowest IAT MSE	01:55	01:50
	Lowest cooling power MSE	02:15	-
08/20 3:00 PM	Lowest IAT MSE	02:10	01:55
	Lowest cooling power MSE	02:55	-

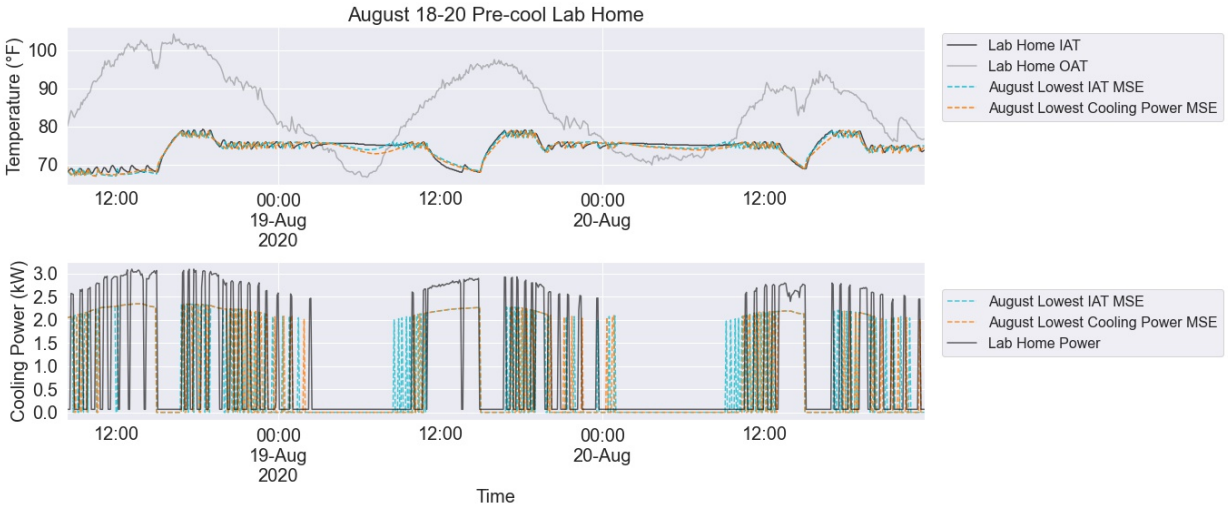

Figure 3. Lowest MSE results comparison during summer period

4.1.2 Winter Calibration

The decay times for the winter pre-heating tests are given in Table 6. Plots for the IAT, OAT, and heating power are in Figure 4. Latent load fraction was not included in the winter calibration because it was a heating test.

The IAT calibration resulted in higher air heat capacities than the heating power calibration, which led to equal or longer decay times for most pre-heating tests. For the first four small pre-heating tests, the IAT calibration average decay time error and the heating power average decay time error was 14 minutes and 11 minutes longer than the dataset, respectively. Both the IAT and heating power calibrations were unable to model the decay rate during the fifth large pre-heating test (December 21st), which decreased the setpoint from 76 °F to 55 °F and resulted in a decay time percent error of -38% and -43% respectively. This large percent error may indicate there were other internal loads contributing to some heat gain not modeled in GridLAB-D, causing a slower decay rate. The GridLAB-D models included all the internal heat gains outlined in the dataset. There may have been some unmeasured heat gains during the December test period contributing to the slow decay rate. The other main difference between the results is that the heating power calibration required higher solar heat gain with the WWR and SHGC multiplied together being larger than the respective values in the IAT calibration. The fifth pre-heating test occurs in the early morning, so the increased solar heat gain does not contribute to a higher internal temperature during that testing period.

The heating electric power plot in Figure 4 shows the combined power from the heat pump and the auxiliary electric furnace. The electric furnace is responsible for the large spikes in power which occur more frequently in the dataset than in GridLAB-D. Some further calibration could be done to increase the usage of the auxiliary heating system in GridLAB-D. The GridLAB-D models show higher electricity consumption when the heat pump is on than the dataset. The nameplate HSPF and heating capacity shown in Table 1 were used in GridLAB-D rather than selecting a heating capacity and COP based on the Lab Homes data. Future work should evaluate other winter heat pump power datasets to understand the difference in power consumption. For the purposes of this study, the timing of the heat pump cycles was more important than the magnitude of the power consumption. The lower air heat capacity value in

the heating power calibration may be from the large power consumption error introduced with the auxiliary heating system. Reducing the air heat capacity makes it more likely the heating system will be on at the same time as when the electric furnace is on in the Lab Home because the heat pump will need to cycle on and off more frequently.

Comparing the winter results to the summer results (see Table 4), the winter parameter combinations required a higher mass heat capacity and lower UA value to match the slow decay rate. The large mass heat capacity and low UA value could be skewed due to the large error during the fifth pre-heating test on December 21st.

Table 6. Decay time during winter period

Pre-heat event	Result type	GridLAB-D decay time (hr)	Lab home decay time (hr)
12/17 6:00 AM	Lowest IAT MSE	02:05	02:00
	Lowest heating power MSE	02:10	-
12/18 6:00 AM	Lowest IAT MSE	01:30	01:05
	Lowest heating power MSE	01:20	-
12/19 6:00 AM	Lowest IAT MSE	03:00	03:00
	Lowest heating power MSE	03:00	-
12/20 6:00 AM	Lowest IAT MSE	01:30	01:05
	Lowest heating power MSE	01:25	-
12/21 12:00 AM	Lowest IAT MSE	08:35	13:45
	Lowest heating power MSE	07:50	-

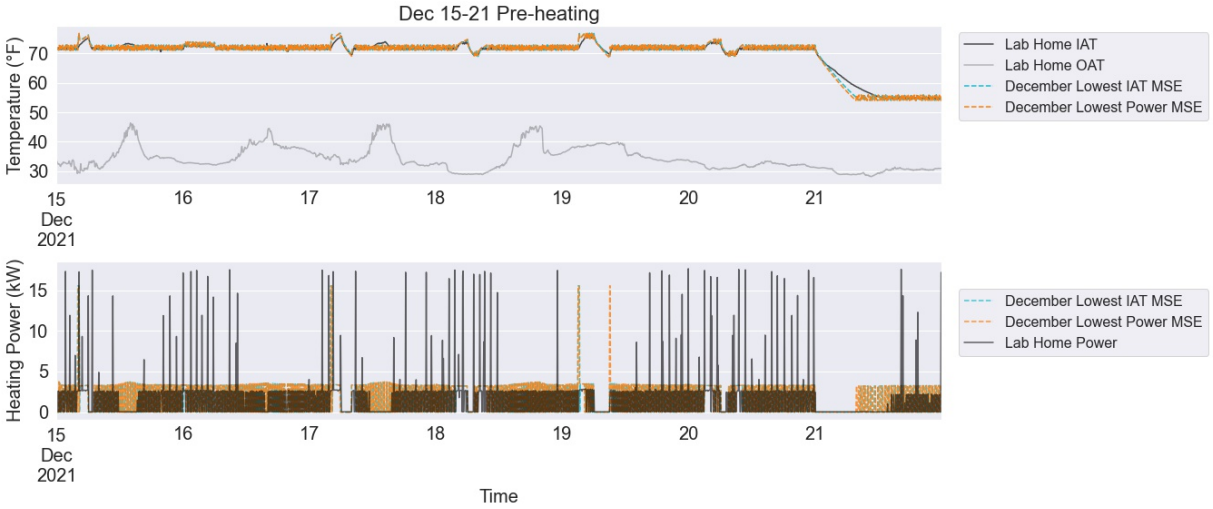

Figure 4. Lowest MSE results comparison during winter period

4.1.3 Spring Calibration

The rise times for the spring pre-cooling and free-floating temperature tests are provided in Table 7. Plots of the IAT, OAT, and cooling power are in Figure 5.

In Figure 5, on June 10th from 7:40 AM to 12:10 PM there is a gap in data from the Lab Home for the IAT. That time period was excluded from the IAT calibration, but because power data was available for that period, the time period was included in the cooling power calibration. The IAT calibration required a higher air heat capacity but a lower overall envelope conductance and SHGC (Table 4). This parameter combination yielded longer rise times when the outdoor air temperature was high, such as in the first pre-cooling test on June 9th. The IAT calibration rise time for the first (June 9th) and third (June 11th) tests were within 4% of the Lab Home data. The rise time for the second pre-cooling test on June 10th was less than half as long as the Lab Home data (5 hours for GridLAB-D and 12 hours for the Lab Home data) for both MSE calibrations.

The high heat capacity and higher integrity envelope in the IAT calibration, resulted in less than half the energy use compared to the Lab Home dataset. Once the thermostat setpoint was met, the house required less energy to maintain the indoor air temperature for the lowest IAT MSE parameter set. The cooling power calibration parameter set included a higher overall UA value and SHGC which resulted in increased external heat gains. Because the temperature was so mild during the spring test period, the impact of the lower envelope integrity is less pronounced in the rise time results in Table 7. The lower integrity envelope in the cooling power calibration results in a more thermally responsive indoor air temperature, demonstrated in Figure 5. The cooling power MSE and IAT MSE metrics alone may not be appropriate for calibrating the thermal dynamics of a house during mild outdoor air temperatures because the minimal drift in indoor air temperature from the setpoint limits possible error in cooling requirements or in indoor air temperature. Therefore, when identifying a best overall parameter set, the spring parameter set was weighted less than the summer and winter calibrations (spring at 0.2, and summer and winter each weighted at 0.4). The afternoon of June 12th through June 13th offer a free-floating temperature test and shows that GridLAB-D models the thermal dynamics of the house well when the heat pump is off during mild outdoor air temperatures.

The latent load fraction for the IAT calibration and cooling calibration were 5% and 15%, compared to 5% and 10% required in the summer results. The relative humidity during the spring dataset ranged from 18.91% to 98.21%, whereas it ranged from 11.69% to 78.81% during the summer dataset. However, as mentioned previously in Section 2.1, GridLAB-D adjusts the latent load fraction based on the relative humidity and reduces the sensible cooling capacity accordingly. For the spring dataset, the adjusted latent load fraction for the 15% rated latent load resulted in a latent load fraction of around 20% during most of the simulation period. Without a moisture balance, it is difficult to determine if 20% is an appropriate latent load fraction. The summer simulation resulted in an adjusted latent load of less than 10% and 15% (for the two rated latent load fractions) when the cooling system was on. The increased latent load fraction in the spring power calibration could be due to the underestimation of the cooling power. The energy error is underestimated in both the power calibration and the IAT calibration. The cooling power calibration is related to the simulation period energy error. Increasing the latent load fraction causes the heat pump to run for longer periods of time to deliver the same sensible cooling and increases the total energy consumption.

Table 7. Rise time during spring period

Pre-cool event	Result type	GridLAB-D rise time (hr)	Lab home rise time (hr)
06/09 02:00 PM	Lowest IAT MSE	05:10	05:00
	Lowest cooling power MSE	03:30	-
06/10 02:00 PM	Lowest IAT MSE	04:55	12:00
	Lowest cooling power MSE	05:00	-
06/11 02:00 PM	Lowest IAT MSE	05:10	05:00
	Lowest cooling power MSE	04:55	-

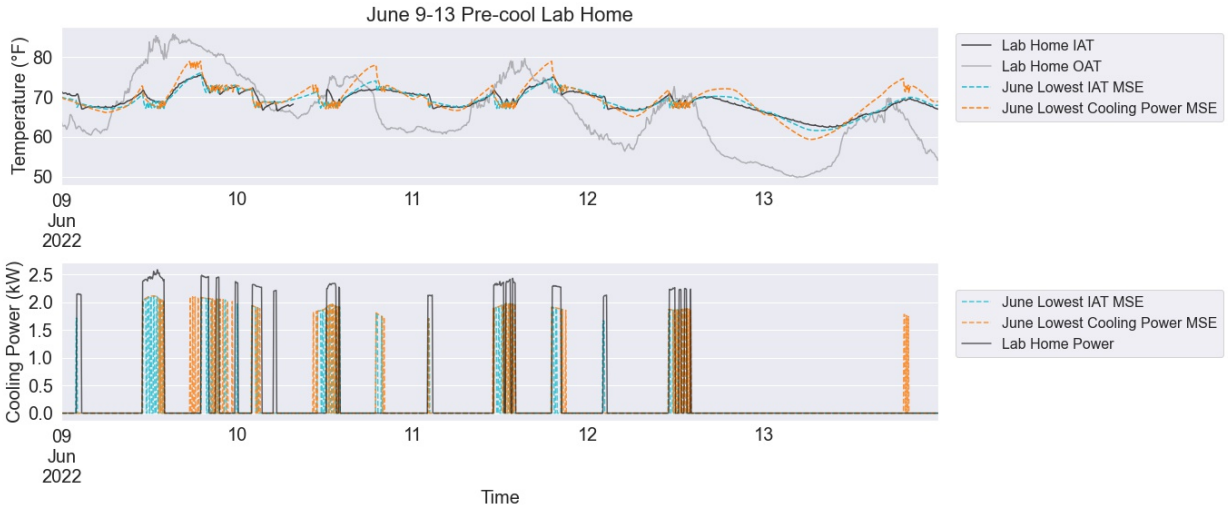

Figure 5. Lowest MSE results comparison during spring period

4.1.4 Overall Calibration

The overall calibration was calculated by completing a parameter grid search for all three seasons using the parameters outlined in Table 2 and weighting the summer, winter, and spring MSE by 0.4, 0.4, and 0.2 respectively. The best options across both MSE metrics (IAT and HVAC electric power) were high integrity envelopes and higher mass heat capacities which could be due to the higher MSE in the winter dataset (see Table 4). Tables 8, 9, and 10 show the rise/decay times for the overall calibration.

The decay and rise time for the IAT calibration studies are well aligned with data in the winter and spring. The rise times for the IAT calibration in the summer is overestimated due to the higher air and mass heat capacities and the lower UA value and solar heat gain compared to the season specific calibration discussed in Section 4.1.1. The HVAC power calibration studies provide better results than the IAT calibration in terms of rise/decay time. The overall calibration for HVAC power closely matches the decay times in December of the IAT calibration and the Lab Home data. The overall calibration for IAT and HVAC power resulted in shorter rise times in the spring for one of the three pre-cooling periods, but as previously discussed in Section 4.1.3, using power or IAT as the sole calibration parameter for periods when the outdoor air temperature is mild, does not produce clear findings. The overall calibration for HVAC power resulted in a slight overestimation of the rise times in the summer pre-cooling dataset but less so than the IAT calibration parameter set. This was likely due to the increased SHGC and smaller air heat capacity compared to the IAT calibration. The absolute energy error is less than 10% for both calibrations. From analyzing the rise/decay time results and the overall goal of this study to accurately simulate the thermal dynamics of a house during setpoint changes, the overall HVAC power calibration is the recommended parameter set.

Table 8. Rise time during summer period for overall recommendation

Pre-cool event	Result type	Simulation rise time (hr)	Lab home rise time (hr)
08/18 3:00 PM	GLD Lowest IAT MSE	03:45	01:50
	GLD Lowest cooling power MSE	02:35	-
	Default	01:10	-
08/19 3:00 PM	GLD Lowest IAT MSE	04:10	01:50
	GLD Lowest cooling power MSE	03:10	-
	Default	01:20	-
08/20 3:00 PM	GLD Lowest IAT MSE	04:00	01:55
	GLD Lowest cooling power MSE	02:50	-
	Default	01:35	-

Table 9. Decay time during winter period for overall recommendation

Pre-heat event	Result type	GridLAB-D decay time (hr)	Lab Home decay time (hr)
12/17 6:00 AM	Lowest IAT MSE	02:10	02:00
	Lowest heating power MSE	01:55	-
	Default	00:45	-
12/18 6:00 AM	Lowest IAT MSE	01:30	01:05
	Lowest heating power MSE	01:20	-
	Default	00:00	-
12/19 6:00 AM	Lowest IAT MSE	03:00	03:00
	Lowest heating power MSE	03:15	-
	Default	01:30	-
12/20 6:00 AM	Lowest IAT MSE	01:30	01:05
	Lowest heating power MSE	01:30	-
	Default	00:05	-
12/21 12:00 AM	Lowest IAT MSE	08:30	13:45
	Lowest heating power MSE	08:10	-
	Default	03:15	-

Table 10. Rise time during spring period for overall recommendation

Pre-cool event	Result type	GridLAB-D rise time (hr)	Lab home rise time (hr)
06/09 02:00 PM	Lowest IAT MSE	05:05	05:00
	Lowest cooling power MSE	05:05	-
	Default	02:40	-
06/10 02:00 PM	Lowest IAT MSE	05:05	12:00
	Lowest cooling power MSE	05:10	-
	Default	03:55	-
06/11 02:00 PM	Lowest IAT MSE	04:55	05:00
	Lowest cooling power MSE	04:50	-
	Default	03:35	-

4.2 GridLAB-D Default Model

Simulations using the default GridLAB-D parameter values (see Section 3.3.2) are compared with the parameter grid search overall calibration in Figures 6 and 7. Table 4 includes error metrics for the default model. The rise/decay times for the default model are outlined in Tables 8, 9, and 10 compared with the overall parameter grid search calibrations. The rise/decay times were not used directly during the calibration process and therefore comparison of the rise/decay time is only a supplemental method of determining the accuracy of the model.

The default GridLAB-D assumptions resulted in a much more thermally responsive model due to the higher UA value and lower mass heat capacity, especially over long periods when the heating or cooling system was off. Rise/decay times across all three seasons were underpredicted. The high UA value significantly impacted accuracy of the rise times during the winter test period. The heating capacity was set to the same value as the calibrated model and matches the namplate data. The rated heating capacity was not able to overcome the increased heat loss through the envelope at lower outdoor air temperatures due to the higher UA value. Although this problem could be solved with autosizing the heating capacity, that would lead to an overprediction of electricity used for heating. The differences between the calibrated model and the default model are more pronounced during very high or very low outdoor air temperatures, indicating that calibrating building models for resilience or extreme weather studies is important.

The default GridLAB-D model assumed a rated latent load fraction of 30% which is likely too high for this climate. During the August time period (Figure 6), the default model took longer to reduce the air temperature down to the lower thermostat setpoint than in the calibrated model. The higher rated latent load fraction contributed to this behavior because it reduced the sensible cooling capacity. The longer heat pump runtimes were also due to the higher UA value than the calibrated model. Given the low humidity climate of Richland, WA, the 10% rated latent load fraction in the calibrated model indicates more of the cooling capacity should be used for sensible cooling than the default assumption. The default assumption for the latent load fraction merits further investigation in higher humidity climates.

The default parameter set resulted in a HVAC power MSE slightly less than the calibrated model. The primary reason for the higher HVAC power MSE in the calibrated model is the auxiliary heating power during the winter. The auxiliary electric furnace never turned on in the default parameter simulation. Because the auxiliary electric furnace consumes 15 kW of electricity when running, if the furnace is not on at the same time as the dataset then it significantly inflates the MSE. In the calibrated model, the electric furnace was on for a total of 10 timesteps (5-minute timesteps). When the 10 timesteps were excluded from the HVAC power MSE calculation, the MSE dropped to 4.32 kW^2 or about 3% less than the default parameter set HVAC power MSE. More calibration could be done on the auxiliary heating controls to lower the HVAC power MSE further. The overall calibration for IAT reduced the IAT weighted MSE by 61% compared to the default assumptions.

The overall calibration for HVAC power was selected as the recommended parameter set given the rise/decay time errors (as discussed in Section 4.1.4). The overall calibration for HVAC power reduced the HVAC total electricity error significantly from the default assumptions. Because of the higher latent load fraction and UA value in the default model, more electricity was required to maintain the indoor air conditions compared to the calibrated model.

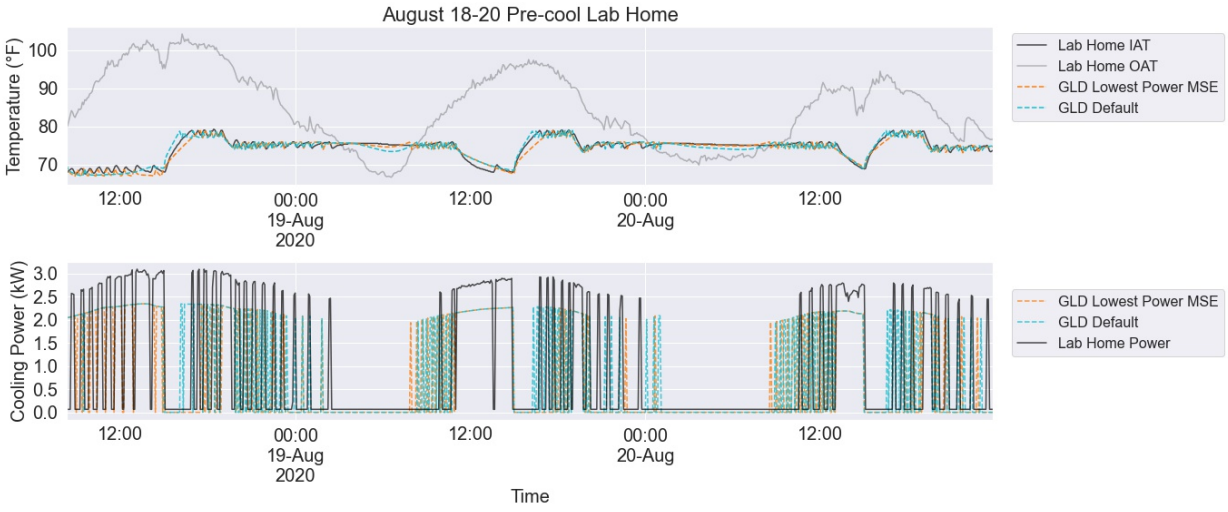

Figure 6. Overall recommendation and default comparison during summer period

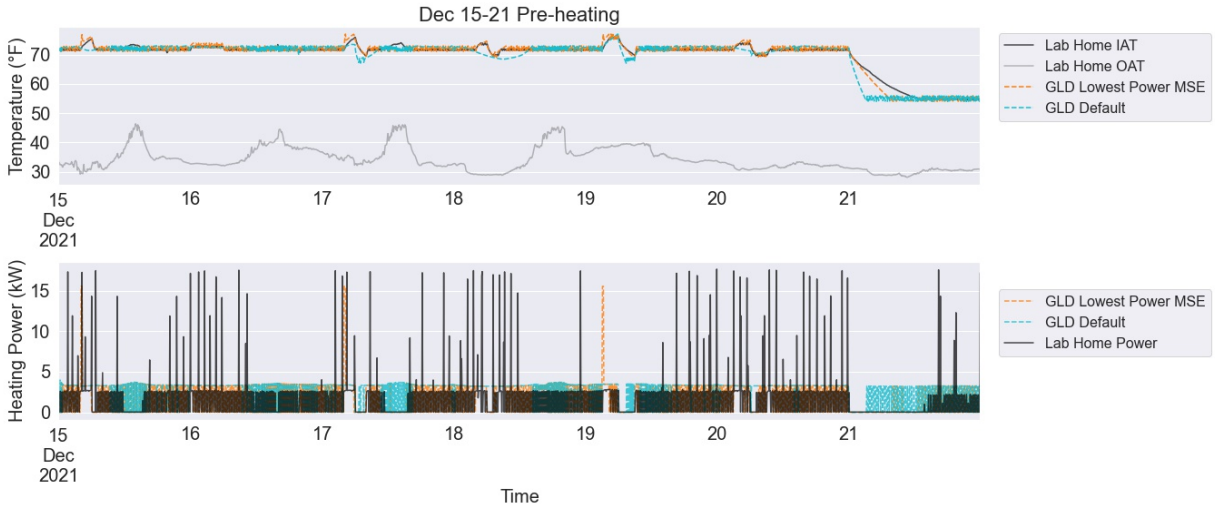

Figure 7. Overall recommendation and default comparison during winter period

4.3 Sensitivity Analysis

A benefit of a parameter grid search is to visualize trends and sensitivities of each parameter for various outputs. The sensitivity analysis started with the overall HVAC electric power calibration parameter set as the baseline and evaluated the adjustment of individual parameters. For example, the air heat capacity was modified from the calibrated parameter set while the other parameters remained at the overall HVAC electric power calibration settings. The various parameter settings were compared by evaluating the HVAC electric power MSE for August and December and the rise/decay time error for August and December datasets. Note, the MSE used here is not weighted for the three seasons like during calibration. The sensitivity analysis uses the MSE across the August and December datasets only (the average of the summer and winter MSE).

4.3.1 HVAC Electric Power MSE Sensitivity

Figure 8 outlines the impact of each parameter on the HVAC electric power MSE for the August and December Lab Home data. The HVAC electric power calibration was selected for the overall calibration and the baseline for the sensitivity analysis. Modifications from the calibrated parameter set only increased the HVAC electric power MSE.

The air heat capacity parameter analysis resulted in a power MSE, averaged across August and December, ranging from 5.59 kW^2 (calibrated parameter) to 5.77 kW^2 (1200 BTU/°F air heat capacity). The air heat capacity impacts the number of heat pump cycles and also minimally contributes to the rise/decay time. The default air heat capacity increased the power MSE by about 1.5%. When the air heat capacity was set to 1200 BTU/°F, the power MSE increased by about 3%. This could be due to the higher air heat capacity contributing to longer rise/decay times during temperature float periods, reducing the need for heating or cooling. The default air heat capacity value results in the worst power MSE in the summer and the second best power MSE in the winter. It's difficult to explain this inconsistent behavior because the air heat capacity affects the timing and length of the heat pump cycles. Small shifts of the heat pump cycles can significantly impact the power MSE. Analyzing the air heat capacity with more data would likely lead to more definitive conclusions. Modifying the air heat capacity only impacts the average power MSE by a maximum of 3% indicating the calibration is not very sensitive to the air heat capacity. Given that a 1000 BTU/°F air heat capacity resulted in the lowest power MSE in the summer and winter, future work should continue to validate GridLAB-D's default air heat capacity assumptions with other building data.

The mass heat capacity parameter analysis resulted in a power MSE ranging from 5.59 kW^2 (calibrated parameter) to 6.14 kW^2 (default mass heat capacity value of 2539 BTU/°F). The general trend indicates that as the mass heat capacity increased, the power MSE decreased until the calibrated parameter of 4180 BTU/°F was reached. The 4180 BTU/°F resulted in the lowest power MSE because the winter test period required longer decay time periods. In the summer, the 4180 BTU/°F mass heat capacity resulted in only a slightly higher power MSE than 3980 BTU/°F (which had the lowest power MSE in the summer). A lower mass heat capacity was slightly better in the summer because the calibrated model overpredicted the rise times (with the 4180 BTU/°F mass heat capacity). A mass heat capacity of 4180 BTU/°F generalizes well across all seasons given the small difference in the power MSE. The default value of 2539 BTU/°F significantly increased the power MSE. The default value originates from an assumption for the total mass per floor area of a residential wood frame construction home. The default mass heat capacity is clearly too low for the PNNL Lab Home even though it does not have particularly massive construction. Modifying the mass heat capacity only increases the power

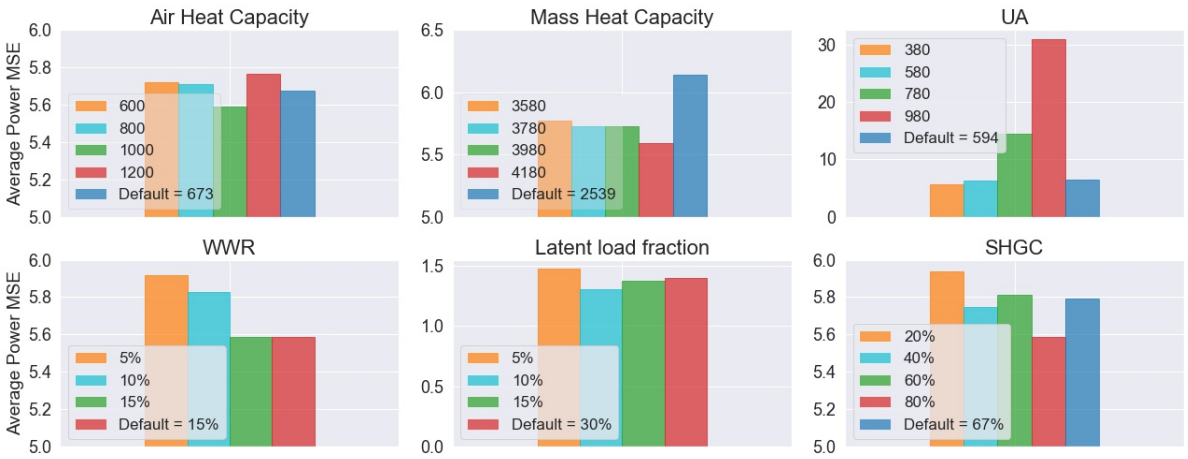

Figure 8. Electric Power MSE Sensitivity Analysis

MSE by about 2% when the mass heat capacity is reduced to 3780 BTU/°F or 3980 BTU/°F. The power MSE is not significantly sensitive to changes to the mass heat capacity.

The electric power MSE was most sensitive to changes to the UA value (the envelope thermal integrity). As the UA value increased, the power MSE increased due to increased heat pump usage to meet the thermostat setpoint. The power MSE exponentially increases as the UA value increases. The increased power MSE mostly originated from the winter dataset which required a lower UA value to maintain the indoor air temperature, particularly during the long decay period. However, the summer period also showed an exponential increase in the power MSE as the UA value increased, further validating the overall calibration value of 380 BTU/°F-hr. The value from the Thermal Parameter Study (Rogers and Brambley 2021) (580 BTU/°F-hr) increased the power MSE by 13% showing the importance of using multiple seasons to determine thermal parameters of buildings. The Thermal Parameters Study UA value included solar heat gains as well which explains the higher number.

The WWR parameter analysis resulted in a power MSE ranging from 5.59 kW^2 (calibrated parameter) to 5.92 kW^2 (WWR of 5%), an increase of 5.8%. Similarly, the SHGC parameter analysis resulted in a power MSE ranging from 5.59 kW^2 (calibrated parameter) to 5.94 kW^2 (WWR of 5%), an increase of 6.2%. In general, as the solar heat gain decreased, the power MSE increased. The one exception was when the SHGC was set to 40% or when the solar heat gain was set to half of the calibrated model's solar heat gain. Given the small dataset, the power MSE was very sensitive to shifts in every heat pump cycle. Testing against more datasets would likely result in more consistent behavior, as indicated by the various WWRs tested and other SHGCs tested. The calibrated parameters were clearly the best and are in agreement with the PNNL Lab Home characteristics.

The latent load parameter analysis shows the summer power MSE only because the latent load isn't incorporated in the winter modoel. Varying the latent load fraction minimally impacted the power MSE which is due to the dry climate of Richland, WA. However, the default rated latent load fraction of 30% increased the power MSE by 6%, emphasizing that the rated latent load fraction should be adjusted based on the climate.

It is important to note the summer model was more sensitive to changes to the thermal parameters than the winter model. This was due to the large power error introduced by the auxiliary heating in the winter which was minimally impacted by changes to the thermal parameters.

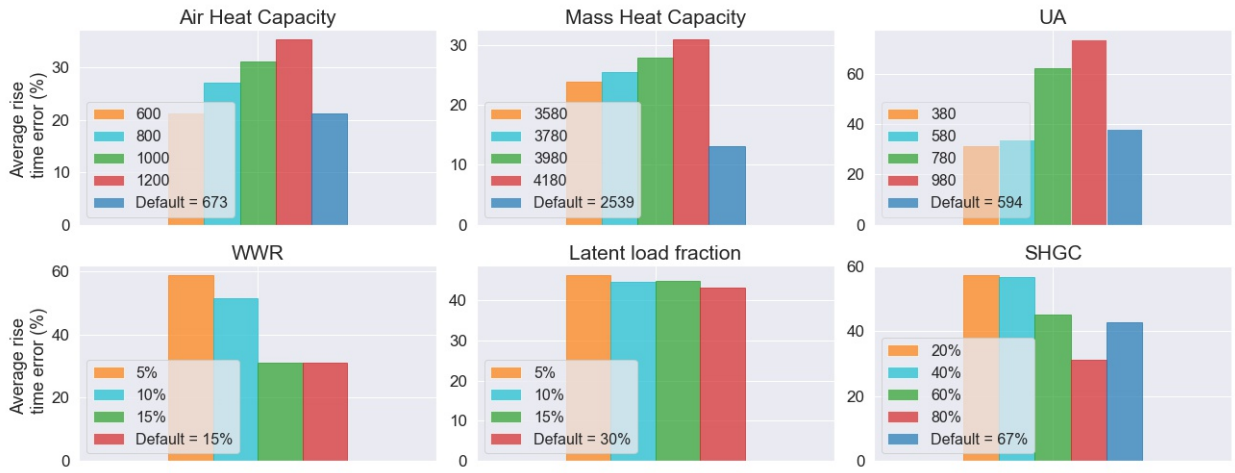

Figure 9. Rise/Decay Time Sensitivity Analysis

4.3.2 Rise/Decay Time Error

Figure 9 outlines the impact of each parameter on the absolute rise/decay time error against the Lab Home data. The rise/decay time error is less straightforward because the calibration was completed using the HVAC electricity MSE across the entire testing period so accurate rise/decay times were a secondary outcome.

The lowest rise/decay time error for the air heat capacity sensitivity analysis occurs when the air heat capacity was set to the default value of 673 BTU/°F, lower than the overall calibration parameter choice of 1000 BTU/°F. Error in rise/decay time decreased slightly as the air heat capacity decreased. The rise and decay times were overpredicted in the calibrated model for the shorter floating temperature tests, as indicated in Tables 8 and 9. By reducing the air heat capacity, the rise and decay times for the shorter floating temperature tests decreased, more closely matching the PNNL Lab Home dataset. Reducing the air heat capacity minimally impacts the already large error in the last pre-heating test. The average rise/decay time error was slightly higher when the air heat capacity was set to 600 BTU/°F compared to the default value of 673 BTU/°F. This discrepancy is likely due to the small dataset size.

Reducing the thermal mass capacity (in the air or mass) improved the rise/decay time accuracy for the shorter periods. The mass heat capacity sensitivity analysis showed a similar trend to the air heat capacity sensitivity analysis. The rise and decay time error decreased as the mass heat capacity decreased (with the default and lowest mass heat capacity having the lowest error).

The UA value rise/decay time error plot shows that as the heat transfer through the building envelope decreased, the rise and decay time error decreased. When evaluating each rise/decay time period individually, there appears to be a switch point between 380 BTU/°F-hr and 580 BTU/°F-hr where the rise/decay times would be better predicted. When the UA value was set to 380 BTU/°F-hr, the rise/decay times were typically overpredicted (expect in the last pre-heating test). When the UA value was set to 580 BTU/°F-hr, the rise/decay times were all underpredicted, indicating the optimal UA value to accurately model the rise/decay times was between 380 BTU/°F-hr and 580 BTU/°F-hr. The 380 BTU/°F-hr used in the calibrated model reduced the rise/decay time error by only 3% compared to the 580 BTU/°F-hr UA value.

The rise/decay time error decreased as the WWR increased which is in line with the SHGC.

When the SHGC increased, the rise/decay time error decreased. Increasing the WWR or the SHGC increases the solar heat gain and shortened the rise time in the summer. The HVAC power calibration already overpredicted the rise time in the summer, so reducing the solar heat gain would only worsen the rise time error. A lower solar heat gain from reduced WWR or SHGC in the winter shortened the decay time marginally. The short pre-heating tests occurred at 6 AM, when indicident solar radiation was relatively low. The long pre-heating test occurred at 12 AM when there was no solar heat gains. Therefore, the sensitivity analysis for the rise/decay time error primarily depended on the summer test period.

The latent load fraction sensitivity analysis for rise time is shown in Figure 9 for August only. Because only August was used for the latent load analysis, it is a small dataset and therefore more difficult to identify trends. The 30% latent load fraction (default) resulted in the lowest rise time error. As the latent load increased, the heat pump's sensible cooling capacity went down and the indoor air temperature was not brought down as far as the model with a lower latent load fraction, shortening the rise time. The rise times across the latent load fractions tested were all within 5 to 10 minutes of each other, so latent load fraction had a minimal effect on the rise time. Latent load fraction in GridLAB-D only impacts the indoor air temperature when the heat pump is on. Rise time is minimally affected if the indoor air temperature reaches its pre-cooling setpoint.

Overall, the rise/decay time was most sensitive to the UA value, WWR, and the SHGC. Although adjustments to the mass heat capacity and air heat capacity affected the rise/decay time, selecting the correct value from a list of reasonable values did not impact the error significantly compared to other parameters. Selecting the incorrect UA value, WWR, or SHGC resulted in greater than a 30% error in rise/decay time.

4.4 Discussion

GridLAB-D is able to capture the thermal dynamics of a residential house model within an acceptable degree of error. In general, the default assumptions in GridLAB-D for the mass heat capacity and latent load fraction may require modification in the future as those two parameters are not typically set by the user initially. The air heat capacity in the overall calibration was increased by 78% from 672.6 BTU/°F to 1200 BTU/°F for the IAT overall calibration and 50% from 672.6 BTU/°F to 1000 BTU/°F for the HVAC power overall calibration. The user sets the mass heat capacity by assigning a total thermal mass per floor area value which automatically subtracts the calculated air heat capacity. The air heat capacity calculation method warrants further validation. The DSO+T study Reeve et al. 2022, randomly chose a thermal mass per floor area value which, for this study, would range from 3734 BTU/°F to 5975 BTU/°F. When the air heat capacity is subtracted from the total thermal mass, the mass heat capacity would range from 3061 BTU/°F to 5302 BTU/°F. The overall calibration assigned a mass heat capacity 4180 BTU/°F which is within the DSO+T study range. The mass heat capacity is likely correctly assigned but further validation with various building envelope materials would validate the upper limit and lower limits of the range. The DSO+T study indicated there is very little building survey data thermal mass. Once the mass heat capacity values are validated, improving the understanding of the distribution of the residential mass heat capacity is required to appropriately capture population loads. The GridLAB-D default assumption of 2539 BTU/°F was too low even though the Lab Home does not have particularly massive exterior walls (wood siding). GridLAB-D users may benefit from choosing the thermal mass value from a list that represents various building materials.

The rated latent load fraction's default assignment of 30% was not ideal for the dry Richland, WA climate with generally low latent loads. Although the latent load fraction did not affect the

rise time when the cooling system was off, a higher rated latent load fraction reduced the sensible cooling capacity and increased the cooling power error even during periods of lower relative humidity. It is difficult to evaluate an appropriate rated latent load fraction because the adjusted latent load is not based on a moisture balance. It is recommended that a moisture balance be added to GridLAB-D which will be especially useful in very humid climates.

A variable WWR for each side of the building façade should improve the solar heat gain modeling in the home. Understanding the distribution of window orientation for populations is required to understand if a variable WWR is necessary or if the over- or under-prediction of solar heat gains will cancel out. The constant WWR was not a barrier to calibrate the Lab Home in this study which essentially found an effective WWR to capture the same solar heat gains as a variable WWR. Given this finding, it is unlikely that the constant WWR is the primary cause of the higher diurnal swing discussed in Section 1.0.

In general, accurate model calibration is possible in GridLAB-D (even with limited data). Because the rise/decay times are modeled well throughout the year, GridLAB-D's modeling capabilities are likely not the cause of the high diurnal electric load swing.

5.0 Preliminary Oklahoma Lab Home Calibration

A dataset from a well instrumented home at the University of Oklahoma (OU) was also evaluated for this study but was missing reliable power data and therefore, a full calibration could not be completed. The OU home has a brick exterior and is located in a humid climate, a perfect candidate to further validate the GridLAB-D's thermal mass and latent load modeling. An initial calibration in GridLAB-D for the IAT only is shown in Figure 10. The initial parameters were from the Thermal Parameters Study (Rogers and Brambley 2021) and the default rated latent load of 30% was used as a baseline. GridLAB-D accurately models the IAT when the outdoor air temperature was high during the rise periods. However, when the OAT drops below the IAT, GridLAB-D's model was too thermally responsive. The cooling capacity or latent load also merits investigation. The GridLAB-D model IAT decayed significantly faster than the OU dataset, indicating the sensible cooling capacity is too high (from either an incorrect total cooling capacity or incorrect latent load fraction), or the solar heat gains are too low. Future work includes completing a full calibration of a home similar to the OU home with a high thermal mass exterior in a location with high outdoor relative humidity.

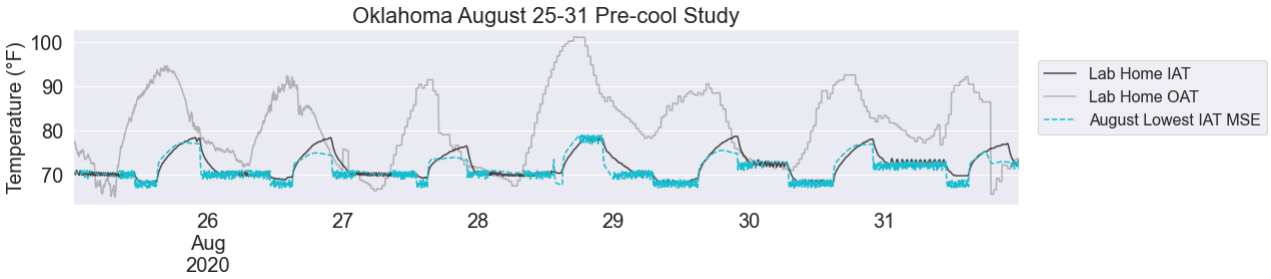

Figure 10. Initial GridLAB-D Model for Home in Oklahoma

6.0 Conclusion

This study investigated how well GridLAB-D's house model characterizes the thermal dynamics of buildings. Modeling thermal dynamics is increasingly important as more demand response and resilience and recovery strategies are modeled in power systems simulation software. Through a parameter grid search, an overall calibration was generated across summer, winter, and spring datasets which included large thermostat setpoint changes to simulate the indoor air temperature changes that may occur at night (and contribute to the diurnal swing in electricity consumption). The calibrated GridLAB-D model (calibrated from HVAC power) resulted in rise/decay times within an average of 22% of the actual home's rise/decay times. For rise/decay time periods less than 5 hours, the calibrated GridLAB-D model was within an average of 16% of the actual home or about 14 minutes.

Although this study validated the GridLAB-D house model is able to capture the home temperature response during relatively large setpoint changes, similar to what occurs with night setback thermostat setpoints, the latent load modeling requires further investigation. The PNNL Lab Homes were chosen as the data source due to data availability that fit the test requirements. Richland, WA is a dry climate and therefore the latent cooling requirement is small. Calibration of the GridLAB-D home with data from a home in a region with high humidity would further prove the need to implement a moisture balance calculation in GridLAB-D's house model. Lastly, the PNNL Lab Homes have wood siding as the exterior wall material which does not substantially increase the thermal mass of the home. The thermal mass of the Lab Homes are primarily inside and is in line with the lumped capacitance method that GridLAB-D uses. The work outlined in this report would benefit from evaluating homes with more massive exterior walls. Information from the sensitivity analysis can be used to decide where to focus on accuracy in the building model definition.

After evaluating the seasonal and overall calibrations, and comparing them with the default GridLAB-D parameter set, grid modelers should feel confident in GridLAB-D's ability to appropriately characterize building thermal dynamics for most homes.

References

Gotseff, P. and Lundstrom, B. 2017. “Data-Driven Residential Load Modeling and Validation in GridLAB-D”. In: *2017 Ninth Annual IEEE Green Technologies Conference (GreenTech)*, pp. 20–25. DOI: 10.1109/GreenTech.2017.9.

GridLAB-D. 2017. GridLAB-D Residential Module User Guide. URL: http://gridlab-d.shoutwiki.com/wiki/Residential_module_user%27s_guide.

GridLAB-D. 2020. GridLAB-D Main Documentation. URL: http://gridlab-d.shoutwiki.com/wiki/Main_Page.

Hale, E., Horsey, H., Johnson, B., Muratori, M., Wilson, E., et al. 2018. *The Demand-side Grid (dsgrid) Model Documentation*. NREL/TP-6A20-71492. Golden, CO: National Renewable Energy Laboratory. URL: https://www.nrel.gov/docs/fy18osti/71492.pdf.

Metzger, C.E., Zhang, J., Mendon, V.V., and Cort, K.A. 2017. *Modeling Cellular Shades in EnergyPlus*. Technical Report PNNL-27187. Pacific Northwest National Laboratory.

PNNL: Lab Homes. 2022. URL: https://labhomes.pnnl.gov/.

Reeve, H.M., Singhal, A., Tbaileh, A., Pratt, R., Hardy, T., Doty, J., Marinovici, L., Bender, S., Pelton, M., and Oster, M. 2022. *DSO+T: Integrated System Simulation*. PNNL-32170-2. Pacific Northwest National Laboratory.

Rogers, A. and Brambley, M. 2021. *Precooling Test Analysis*. Richland, WA: Pacific Northwest National Laboratory.

Schneider, K. and Fuller, J. 2010. “Detailed end use load modeling for distribution system analysis”. In: pp. 1–7. DOI: 10.1109/PES.2010.5588151.

Sonderegger, R. 1978. *Dynamic Models of House Heating Based on Equivalent Thermal Parameters*. Doctoral Dissertation Report PU/CES 57. Princeton, New Jersey: Princeton University.

Subbarao, K. 1981. *Thermal Parameters for Single and Multizone Buildings and Their Determination from Performance Data*. Golden, Colorado: Solar Energy Research Institute.

Wilson, N.W., Wagner, B.S., and Colborne, W.G. 1985. “Equivalent Thermal Parameters for an Occupied Gas-Heated House”. In: *ASHRAE Transactions* 91 (Part 2).

Zhou, X., Shi, J., Tang, Y., Li, Y., Li, S., and Gong, K. 2019. “Aggregate Control Strategy for Thermostatically Controlled Loads with Demand Response”. In: *Energies* 12.4. ISSN: 1996-1073. DOI: 10.3390/en12040683. URL: https://www.mdpi.com/1996-1073/12/4/683.

Pacific Northwest National Laboratory

902 Battelle Boulevard
P.O. Box 999
Richland, WA 99352
1-888-375-PNNL (7675)

www.pnnl.gov